Structural transition in two-dimensional Hertzian spheres in the presence of random pinning

E. N. Tsiok ⬤, Yu. D. Fomin, E. A. Gaiduk, and V. N. Ryzhov ⬤

Institute of High Pressure Physics RAS, Kaluzhskoe shosse, 14, Troitsk, 108840 Moscow, Russia

Using molecular dynamics simulation we have investigated the influence of random pinning on the phase diagram and melting scenarios of a two-dimensional system with the Hertz potential for $\alpha = 5/2$. It has been shown that random pinning can cardinally change the mechanism of first-order transition between the different crystalline phases (triangular and square) by virtue of generating hexatic and tetratic phases: a triangular crystal to hexatic transition is of the continuous Berezinskii-Kosterlitz-Thouless (BKT) type, a hexatic to tetratic transition is of first order, and finally, there is a continuous BKT-type transition from tetratic to the square crystal.

I. INTRODUCTION

Studying the self-organization of two-dimensional (2D) systems, especially soft or deformable colloidal mesoparticle systems such as dendrimers, star polymers, and block-copolymer micelles [1–3], is of great interest for both fundamental science and technological applications. Of particular interest for optical applications are the structures of crystalline phases and the relation of these structures with the form of interparticle potential. The most popular potentials used to describe deformable nanocolloids are nontrivial phenomenological interactions, some of which even lead to a complete overlap among the components and demonstrate very rich phase behavior [1,4–7]. It seems that the simplest form of the family of these potentials is the Hertz potential [4]. Recently the behavior of 2D Hertzian spheres has been studied in a number of articles [8–12].

In the present article we discuss the influence of disorder on the phase diagram of 2D Hertzian spheres. As far back as in the 1970s it was established that the melting of 2D systems could in principle be different from the melting of three-dimensional (3D) crystals. If in the 3D case melting is always a first-order phase transition, then 2D systems can melt according to several different scenarios (see [13,14] and the references in these works). Today there are known at least three different melting scenarios of 2D systems: first, melting via a first-order phase transition [15,16] and, second, a melting scenario according to the Berezinskii-Kosterlitz-Thouless-Halperin-Nelson-Young theory (BKTHNY) [17–21]. In this scenario melting takes place via two continuous transitions of the Berezinskii-Kosterlitz-Thouless (BKT) type. As a result of the first transition, the long-range orientational order is destroyed in the crystal and transforms into quasi-long-range (power decay of the orientational order correlation functions), and the translational order from quasi-long-range becomes short-range. The obtained phase is called hexatic. The second continuous BKT phase transition leads to a disappearance of the quasi-long-range orientational order, as a result of which

the system changes to isotropic liquid with short-range orientational and translational orders. Finally, the third melting scenario of 2D crystals is as follows: melting also occurs in two stages, but transition from crystal to hexatic is continuous of the BKT type, and from hexatic to liquid is of the first order [22–26]. We will call these scenarios the first, second, and third.

It is significant that in all classical works on studying 2D melting only one crystalline structure was considered, i.e., a triangular crystal that is a close-packed structure in two dimensions. At the same time, recent experimental works have shown the possibility of the existence of other 2D and quasi-2D crystalline structures. A more widely known example is graphene that is a sheet of graphite, i.e., a 2D layer with a honeycomb structure [27]. Later, other 2D and quasi-2D structures were also found, for instance, square ice in water confined in a slit pore [28], a square crystal of iron atoms in the defects of graphene [29], complex crystalline structures in a thin colloidal film [30], and in a system of vortices in superconductors [31,32]. However, up to now obtaining nontriangular 2D crystals is rather an exception than a rule, and the overwhelming majority of 2D systems crystallize exactly into a triangular lattice.

At the same time, nontriangular 2D crystalline lattices have been found in a large number of works on computer simulation of 2D systems, for instance, in a system with two scale-repulsive shoulder potentials [33–38] and in water [39–43]. In [44–48] a square crystal was found, in [47,48] a honeycomb structure was observed, and the Kagome lattice was discovered in [43,49]. In a number of publications formation of quasicrystalline phases in 2D systems was reported [50–53].

Experimental investigation of 2D crystal melting is complicated by the presence of the so-called "pinning" of particles. It means that because of the effects of interaction with the underlayer some particles turn out to be pinned to certain fixed places. It is clear that the presence of pinning and the

concentration of pinned particles may considerably affect a system's behavior.

One should discriminate between the two types of pinning. In the case of quenched disorder, a random fraction of particles could be pinned either to random positions in the system or on lattice sites of the underlying crystal phase. With regard to the pinned particles at random sites, it was shown theoretically that quenched disorder influenced crystalline order but almost did not affect orientational order. So the BKTHNY melting scenario persisted, and the solid phase was destroyed entirely for high pinning fractions (see [54–59]). Experiments and simulations of 2D melting of superparamagnetic colloidal particles with quenched disorder confirmed the increased stability range of the hexatic phase (see [60–62]).

However, in [63] the authors study the melting of a 2D system of hard disks with quenched disorder, which results from pinning random particles on a crystalline lattice. This kind of pinning stabilizes the solid phase and can destroy the hexatic phase. We are not aware of real experiments with this kind of disorder.

Finally, in [64] it was demonstrated that random pinning could qualitatively change the first-order melting scenario—it can generate the hexatic phase and transform the first-order transition into the third type of melting scenario.

As mentioned above, recently a number of 2D systems have been discovered where various crystalline phases exist. It should be noted that in the earlier publications including the seminal articles by Halperin, Nelson [19,20], and Young [21] a triangular crystalline structure was only considered, and now a strict melting theory exists only for this structure. In more recent articles where the new crystalline phases were found the main attention of the authors was focused on the structure of these phases and their melting scenarios. At the same time, the possible structural transitions among these crystalline phases were not discussed at all. It was implicitly supposed that the transformations of these phases with different symmetries occurred as a standard first-order phase transition. However, as was shown in our previous publication [64], random pinning could change one first-order melting transition into two (the third melting scenario in that work) due to generation of the hexatic phase. The question is whether it is possible to see similar behavior in the case of a first-order structural transition. The problem is even more interesting because random pinning will affect both crystalline phases. The main goal of the present article is to investigate the influence of random pinning on the structural transitions in 2D systems.

One of the systems, in which in the 2D case a complex phase diagram with a large number of different phases is observed, is the Hertz model. It is a system of particles that interact through the potential

$$U(r) = \varepsilon(1 - r/\sigma)^{\alpha} H(1 - r), \qquad (1)$$

where $H(r)$ is the Heaviside step function and parameters ε and σ set the energy and length scales. In the case of $\alpha = 5/2$ the Hertz potential corresponds to the energy of deformation of two elastic spheres [65].

The phase diagram of Hertzian spheres with $\alpha = 5/2$ has many different ordered phases in both three dimensions [7,66] and two dimensions [9]. Also, in Hertzian spheres a number

of anomalous properties of liquid are observed (see [66] for the 3D case and [9] for the 2D one).

The phase diagram of 2D Hertzian spheres with $\alpha = 5/2$ was discussed in several publications [9–11]. The most complete calculation of this phase diagram is given in [9], which shows that in this system several stability regions of the triangular crystal are observed, several of the square one as well as a number of other phases including the dodecagonal quasicrystal. In that work as well the melting scenarios of the triangular and square crystals with low density were determined, and it was shown that in this system all three currently known melting scenarios take place. During changing from low to high densities, the melting lines of both triangular and square lattices pass through a maximum, after which the melting temperature begins falling with an increase in density. Moreover, in the region of the reentrant melting curve of the triangular phase there are two tricritical points, in which a change in the melting scenarios takes place from the third to BKTHNY at the maximum and from BKTHNY to the third at lower temperatures. The tricritical point on the melting curve of the square crystal is located at the maximum, in which a change in the transition scenario from the third to a first-order transition takes place.

In the present paper we examine the influence of random pinning on the melting scenario of the triangular and square crystals of 2D Hertzian spheres with $\alpha = 5/2$ and on the transition between these two crystalline phases in the region of reentrant melting at low temperatures. The influence of random pinning on the structural transition has never been considered up to now to the best of our knowledge. As mentioned above, the previous works considered only the influence of random pinning on melting of the triangular crystal where melting occurs according to the first and the third scenarios [58,64]. Therefore studying the behavior of 2D Hertzian spheres at different concentrations of random pinning allows us to solve three problems at once: (1) considering the influence of random pinning on melting of the triangular crystal when the different melting scenarios take place,(2) investigating the influence of random pinning on melting of the square crystal in the two different melting scenarios, and (3) we also demonstrate that random pinning drastically changes the scenario of the structural transition between the triangular and square crystalline phases. In Fig. 1 we summarize the results, which will be discussed in detail below.

II. SYSTEM AND METHODS

In the present paper using a molecular dynamics method within the framework of the software package LAMMPS [67] we simulated a 2D system of Hertzian spheres in the region of low densities, in which the triangular and square phases were observed (see Fig. 1). When investigating the triangular phase, $N = 20\,000$ particles were simulated in a rectangular box, whereas to study the square phase, $N = 22\,500$ particles in a square box were used. In all cases, periodic boundary conditions were applied. The samples of liquid were obtained by melting respective lattices.

The systems were simulated using 60 million steps with time interval $dt = 0.0001$ in NVT and NVE ensembles (NVT for equilibration and NVE for production); the first
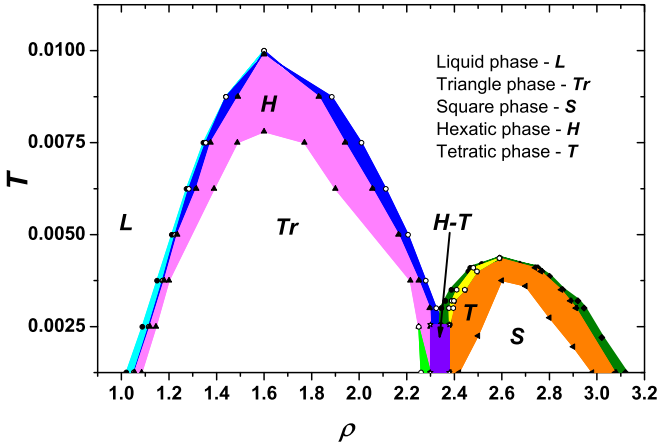
FIG. 1. The full phase diagram of a pure system and of a system with pinning in the area of existence of the triangular and square crystals. (1) Cyan is liquid-hexatic phase coexistence; (2) blue is the hexatic phase without pinning; (3) magenta is the hexatic phase with 0.1% pinning; (4) green is the extension of the hexatic phase for 0.2% pinning; (5) olive is liquid-tetratic phase coexistence; (6) yellow is the tetratic phase without pinning; (7) orange is the tetratic phase with 0.2% pinning; (8) violet is hexatic-tetratic coexistence. See explanations in the text.

30 million steps were used for equilibration. The concentration of pinning particles at random positions varied from 0.1% (the triangular lattice) to 0.2% (the square lattice). We chose these two small values of the concentrations of pinning centers because as was shown in the seminal paper by Nelson [54] (see also [55,56]) a large fraction of pinning sites simply destroyed crystalline order (quasi-long-range translational order) leaving hexatic order (quasi-long-range orientational order) almost unchanged. The previous simulations [58–61,64] showed that a small concentration of pinning centers, 0.1, during the melting of the triangular lattice was sufficient to see the qualitative change of the phase diagram as a result of hexatic phase generation, but the crystal was not destroyed completely. Since the square phase is more resistant to random pinning, we used larger concentration, 0.2 These small concentrations are sufficient to demonstrate the qualitative effect of random pinning on the mechanisms of 2D melting and the structural transitions between the crystalline phases. The procedure of introduction of pinning particles is described in detail in [58,59,64]. We considered not fewer than 10 different systems with various initial random positions of fixed particles with further averaging by these replicas. In the course of simulation, the system pressure was calculated as a function of density and temperature. The transition regions between different phases were determined based on the peculiarities on the equations of state (isotherms) and the Mayer-Wood loop (an analogy of the van der Waals loop for the 3D case), while the structure of these phases was obtained from the radial distribution functions. We also calculated orientational and translational order parameters and their correlation functions to determine the stability limits of the triangular and hexatic phases as well as the square and tetratic (an analogy of hexatic for the square crystal) phases.

The translational order parameter is calculated in the standard way [19,20,59,64]:

$$\psi_t = \frac{1}{N}\left\langle\left\langle\left|\sum_j e^{i\mathbf{G}\mathbf{r}_j}\right|\right\rangle\right\rangle_{rp}. \tag{2}$$

The local orientational parameter is given in the following way [19,20,59,64]:

$$\Psi_{mj} = \frac{1}{N_j}\sum_{k=1}^{N_j} e^{mi\theta_{jk}}, \tag{3}$$

where N_j is the number of the nearest neighbors of particle j that is determined from the Voronoi construction, θ_{jk} is the angle of the bond between particles j and k relative to an arbitrary reference axis, $\mathbf{G}$ is a primary reciprocal lattice vector, and index rp points to averaging by 10 replicas with different initial random positions of the fixed particles. The global orientational order parameter is obtained by means of averaging over all particles

$$\psi_m = \frac{1}{N}\left\langle\left\langle\left|\sum_j^N \Psi_{mj}\right|\right\rangle\right\rangle_{rp}, \tag{4}$$

where $m = 6$ for the triangular lattice and $m = 4$ for the square one.

The orientational correlation function (OCF) is defined as

$$G_m(r) = \left\langle\frac{\langle\Psi_m(\mathbf{r})\Psi_m^*(\mathbf{0})\rangle}{g(r)}\right\rangle_{rp}, \tag{5}$$

where $g(r) = <\delta(\mathbf{r}_i)\delta(\mathbf{r}_j)>$ is the pair distribution function. In the hexatic and tetratic phases the long-range behavior of $G_m(r)$ has the form $G_m(r) \propto r^{-\eta_m}$ with $\eta_m \leqslant \frac{1}{4}$ [19,20].

The translational correlation function (TCF) is calculated as

$$G_t(r) = \left\langle\frac{<\exp[i\mathbf{G}(\mathbf{r}_i - \mathbf{r}_j)]>}{g(r)}\right\rangle_{rp}, \tag{6}$$

where $r = |\mathbf{r}_i - \mathbf{r}_j|$. In the solid phase the long-range behavior of $G_t(r)$ has the form $G_t(r) \propto r^{-\eta_T}$ with $\eta_T \leqslant \frac{1}{3}$ [19,20]. The stability limits of the square crystal were determined in the same way. In the hexatic (tetratic) phase and isotropic liquid $G_t(r)$ decays exponentially.

The presence of random pinning decreases the range of stability of a crystalline phase and consequently relatively expands the area of existence of the hexatic (tetratic) phase, which allows investigating its dynamic properties by means of calculating the diffusion coefficient [59]. To do this Einstein's method was used, i.e., mean-square displacement $<r^2(t)>$ was calculated, which is proportional to time at large times, $<r^2(t)> = 4Dt$, where D is a diffusion coefficient.

III. MELTING OF THE TRIANGULAR CRYSTAL IN THE PRESENCE OF RANDOM PINNING

Let us consider Hertzian spheres with random pinning 0.1% in the melting area of the triangular crystal (see Fig. 1). Recall that random pinning, as a rule, does not practically affect the stability limit of hexatic but significantly decreases the stability area of a crystal. As a result, compared with a
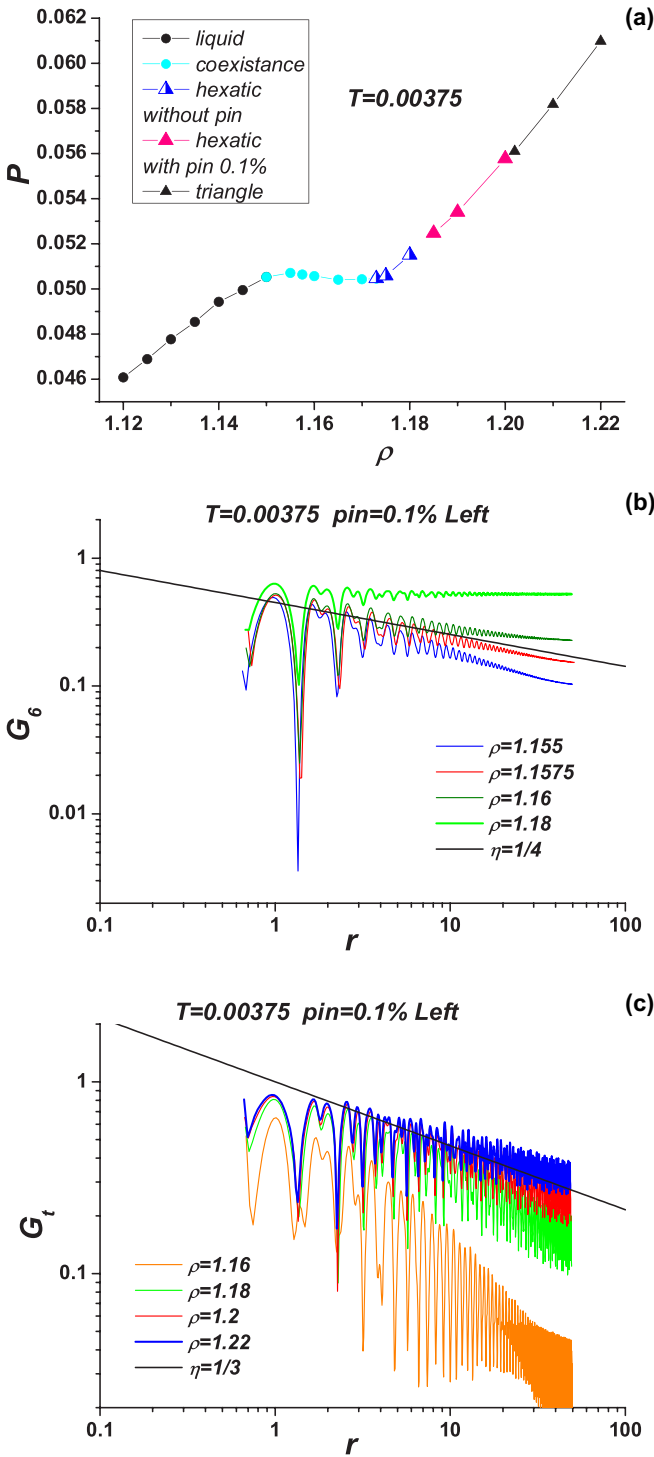
FIG. 2. (a) The equation of state of Hertzian spheres at $T = 0.00375$ with concentration of random pinning 0.1% at the left branch of the triangular crystal melting line. (b) The behavior of OCF G_6 of the same system. (c) The behavior of TCF G_t of the same system.

system without random pinning the area of existence of the hexatic phase relatively increases [9,54–56,58,61,64].

Figure 2(a) presents the system's equation of state on isotherm $T = 0.00375$ at the crossing of the left branch of the triangular crystal melting curve with the Mayer-Wood loop

characteristic of first-order transition. On this isotherm we marked the points of stability loss of the crystal and hexatic obtained from analysis of the orientational and translational order parameter correlation functions shown in Figs. 2(b) and 2(c). From the obtained results it can be concluded that the crystal to hexatic transition is a continuous one of the BKT type, while the hexatic to isotropic liquid transition is a first-order transition. Thus, on the left branch the melting scenario remained the same as in the system without pinning (the third scenario) [9], but the stability limit of the crystal shifted to higher densities, which led to expansion of the hexatic phase existence area.

Figure 3 shows an equation of state without the Mayer-Wood loop and the behavior of the correlation functions at the crossing of the right branch of the triangular crystal melting curve at $T = 0.00375$ (see Fig. 1). In this area in the absence of random pinning the system melts via two continuous transitions of the BKT type in accordance with the BKTHNY theory [9]. We can see that in this case the introduction of random pinning also did not change the transition scenario but only significantly expanded the hexatic phase existence area.

IV. THE INFLUENCE OF RANDOM PINNING ON SQUARE CRYSTAL MELTING

In this part of the paper we address the influence of random pinning on melting of the square crystal in Hertzian spheres. In order that the effect of random pinning becomes more vivid, we increased the concentration of pinned particles to 0.2%. Searching for the distinct boundary between the square crystal and the tetratic phase was carried out similarly to the procedure described above for the triangular crystal.

Figure 4(a) shows the equation of state of the system with random pinning at $T = 0.0032$ at the crossing of the left branch of the square crystal melting line, on which the Mayer-Wood loop was found, and in Figs. 4(b) and 4(c): the orientational and translational order parameter correlation functions for the square crystal are shown. In order to visualize the influence of random pinning on the tetratic phase we also show in Fig. 4(a) the limit of stability of the square crystalline phase without pinning that goes out of the Mayer-Wood loop. In this region without random pinning the crystal to tetratic transition is a continuous one of the BKT type, whereas the tetratic to isotropic liquid transition is a first-order transition [9]. It is evident that in the presence of random pinning the area of tetratic phase existence has significantly expanded without changing the melting scenario, which is in qualitative agreement with the influence of pinning on triangular crystal melting for the third melting scenario.

In Fig. 5 the same analysis is performed for the right branch of the square crystal melting curve. In Fig. 5(a) the equation of state with the Mayer-Wood loop at the crossing of the melting curve right branch at $T = 0.0032$ is shown. Again, we can see a very wide area of the tetratic phase under the influence of pinning, the border of which was determined from the behavior of G_t in Fig. 5(c). Recall that in the system without random pinning this branch melted via one first-order transition [9] (both criteria following from the behavior of G_4 and G_t are inside the Mayer-Wood loop), i.e., in this case we observe a qualitative change in the melting scenario: in the
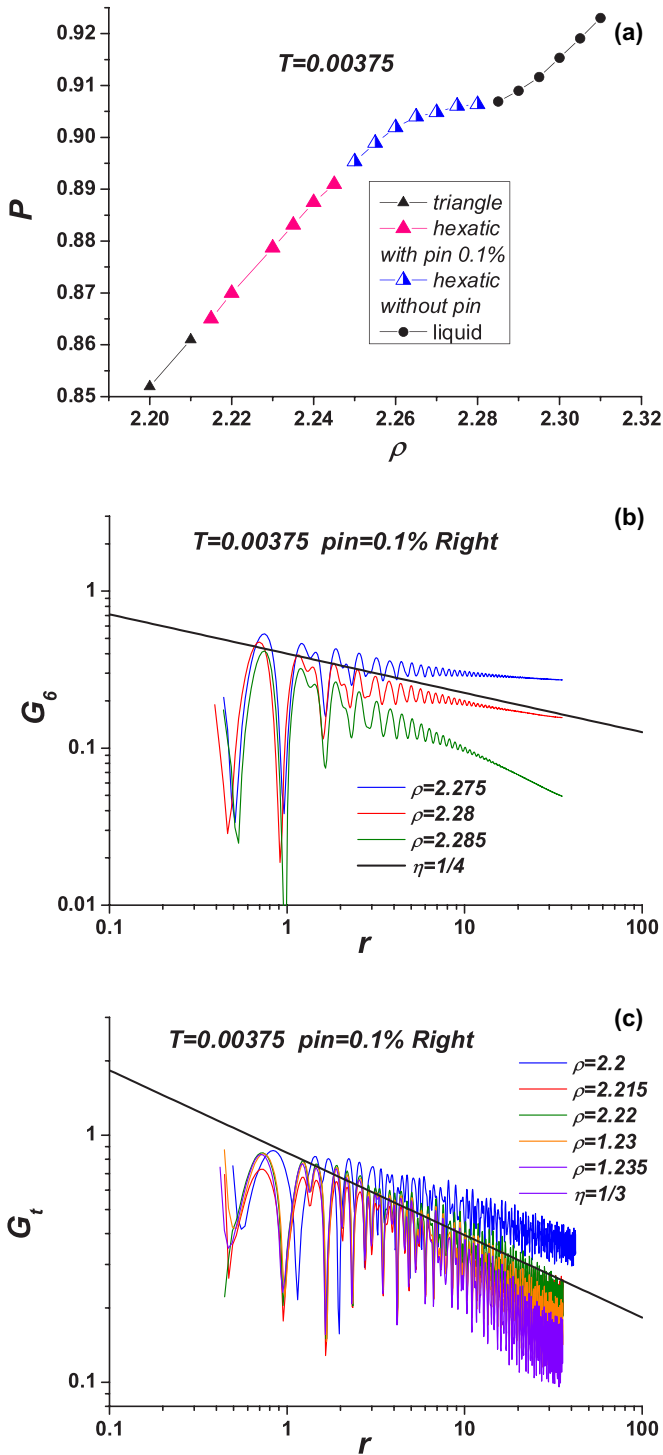
FIG. 3. (a) The equation of state of Hertzian spheres at $T = 0.00375$ with concentration of random pinning 0.1% at the right branch of the melting line of the triangular crystal. (b) The behavior of OCF G_6 of the same system. (c) The behavior of TCF G_t of the same system.
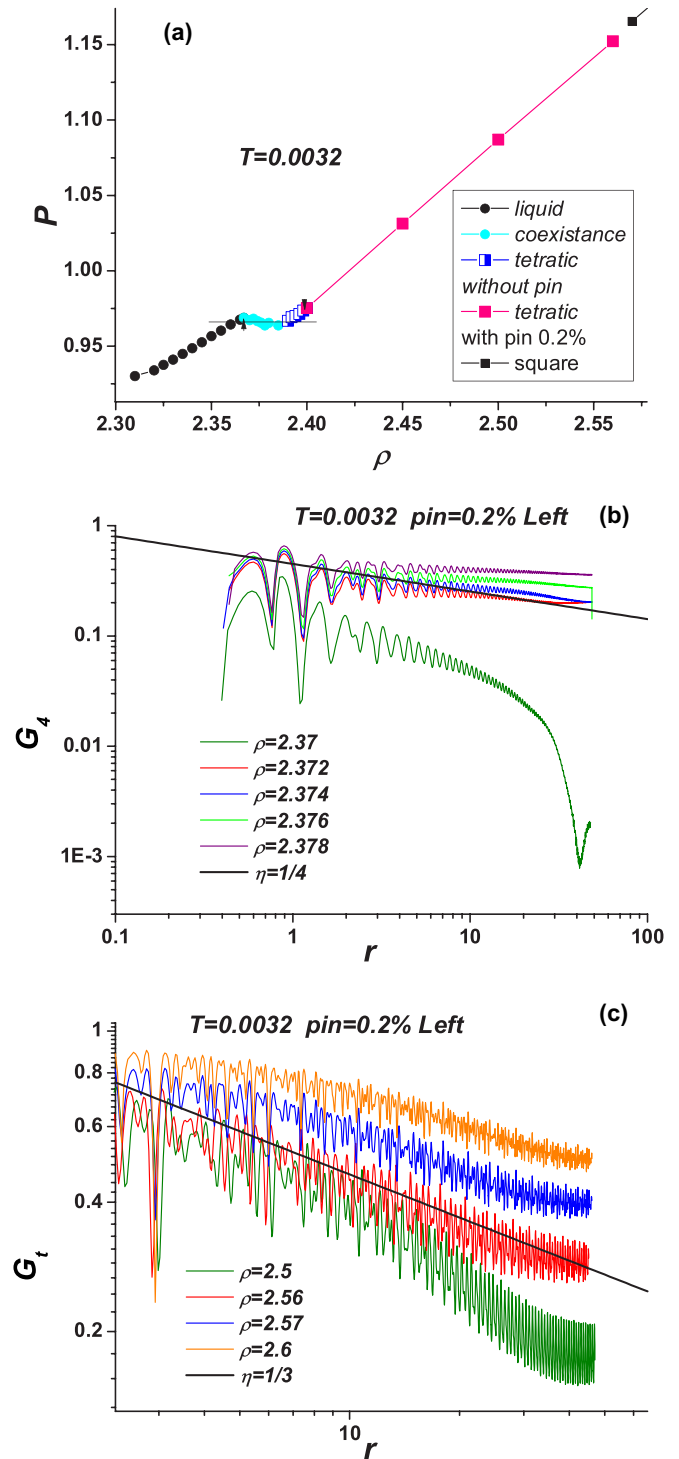

FIG. 4. (a) The equation of state of Hertzian spheres at $T = 0.0032$ with concentration of random pinning 0.2% at the left branch of the melting line of the square crystal; (b) orientational correlation function G_4 at $T = 0.0032$; and (c) translational correlation function G_t along the same isotherm.

presence of random pinning the system melts according to the third scenario.

Thus, the introduction of random pinning significantly influences square phase melting. As in the triangular crystal case, a considerable increase in the tetratic phase existence area occurs. Moreover, if for the left branch the changes are limited to the shifting of the crystal stability line, then in the right one a change in the crystal melting scenario takes place from one first-order transition to the third type of melting.

FIG. 6. The equation of state of Hertzian spheres at $T = 0.00125$ with concentration of random pinning 0.2% at the crossing of the first-order phase transition from the triangular to square crystal as compared with the system without pinning.
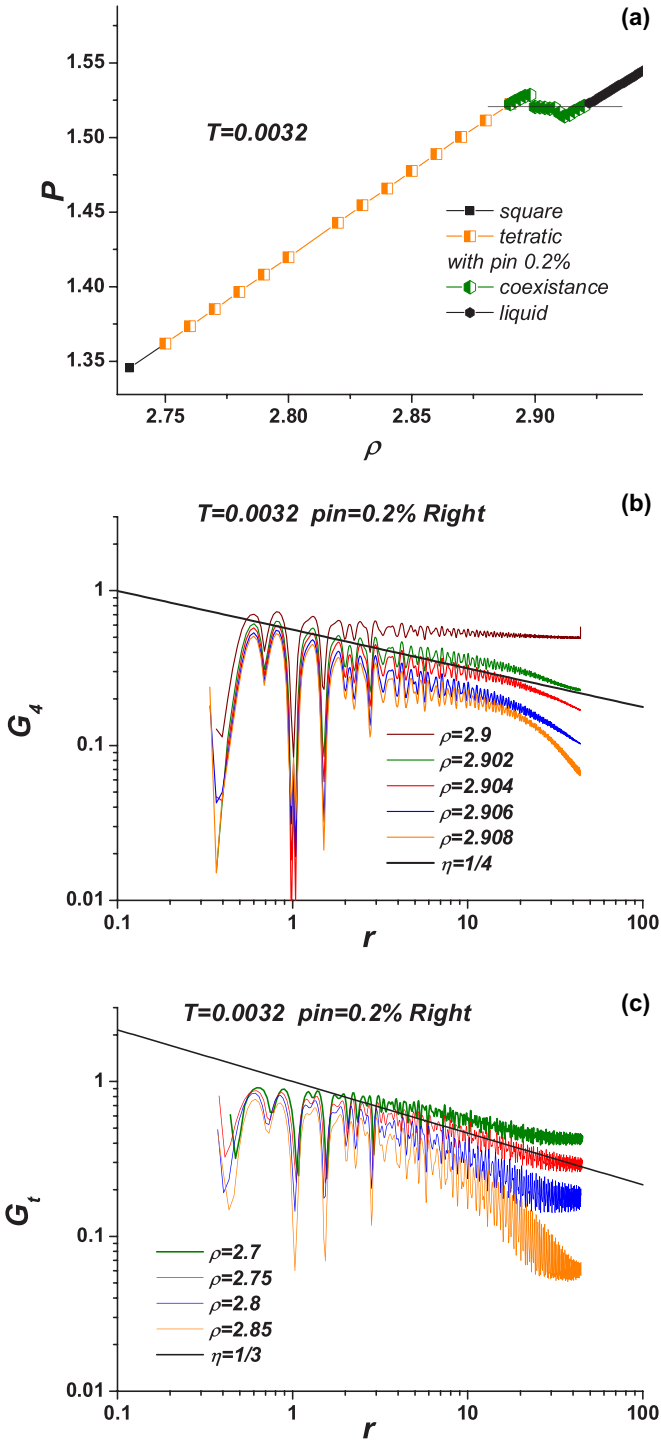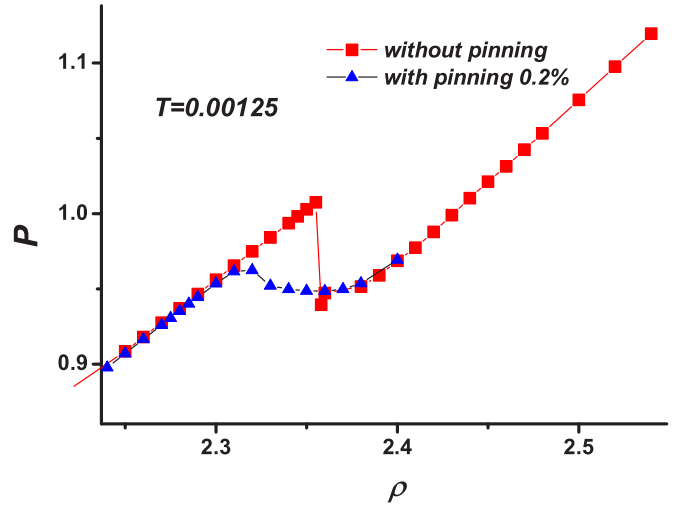

FIG. 5. (a) The equation of state of Hertzian spheres at $T = 0.0032$ with concentration of random pinning 0.2% at the right branch of the square crystal melting line; (b) orientational correlation function G_4 at $T = 0.0032$; and (c) translational correlation function G_t along the same isotherm.

V. THE INFLUENCE OF RANDOM PINNING ON TRANSITION FROM THE TRIANGULAR LATTICE TO THE SQUARE ONE

Above it was shown that random pinning could significantly affect 2D crystal melting. This influence is primarily connected with a considerable growth of the existence areas of the phases that are an intermediary between the crystal and liquid (the hexatic phase for the triangular crystal and tetratic for square). In some cases, this intermediary phase does not exist at all in the system without pinning but appears in its presence [64]. This enables us to suppose that at low temperatures in the neighborhood of transition between two crystals the stability limit of the triangular phase will move to lower densities and that of the square phase will be shifted to higher densities. One can conclude that the structural transition will take place not between two crystals but with the participation of the hexatic and tetratic phases. This is to our knowledge a new mechanism of structural transition in two dimensions in the presence of random pinning. We believe that this mechanism is general and independent of the form of the potential. This part of the paper is devoted to verifying this mechanism. In doing so we will simulate systems with random pinning concentration 0.2%.

Figure 6 shows the equation of state at $T = 0.00125$ in the area of densities that crosses the transition line from the triangular crystal to the square one. For comparison, the results for the system with and without random pinning are shown. It can be seen that in the system without random pinning a sharp fall from one phase to the other takes place in the middle of the two-phase area. Such behavior, to all appearances, is connected with the effects of metastability in transitioning between the two crystals that can be resolved by means of lengthy simulation or by the introduction of defects in the form of random pinning. As can be seen from Fig. 6 in the system with pinning the Mayer-Wood loop already has a smooth standard form.

In order to understand the nature of change of the equation of state along isotherm $T = 0.00125$ under the influence of pinning (Fig. 6) in the metastable area (for instance, to the coexistence of what phases will it correspond?) and beyond it let us consider the correlation functions of translational and orientational order for the triangular lattice to the left of the
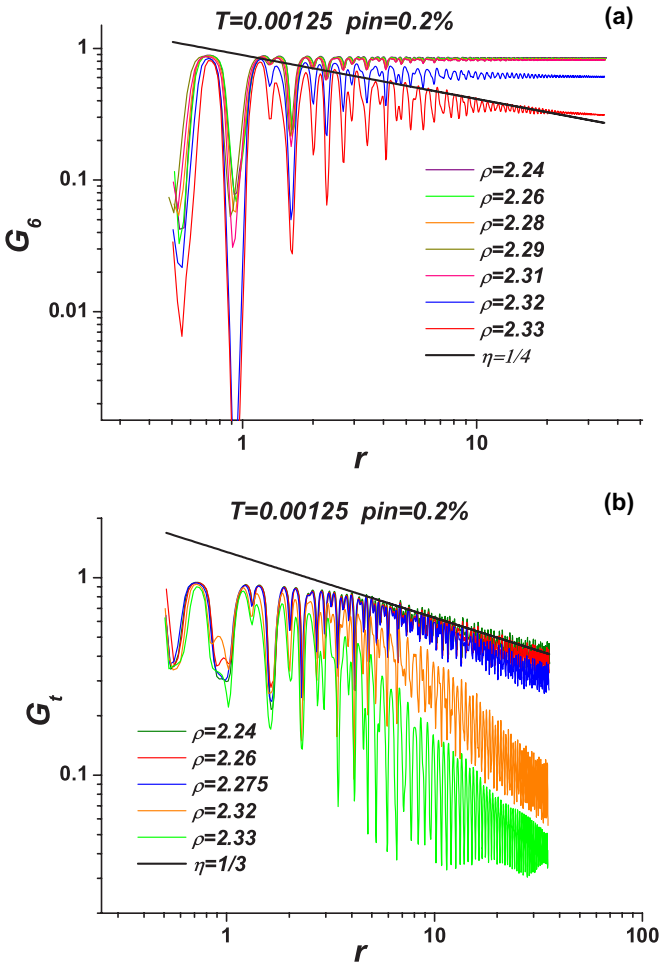
FIG. 7. (a) The orientational and (b) translational correlation functions with the symmetry of a triangular lattice with concentration of random pinning 0.2% in the region of transition from the triangular to square crystal at $T = 0.00125$.
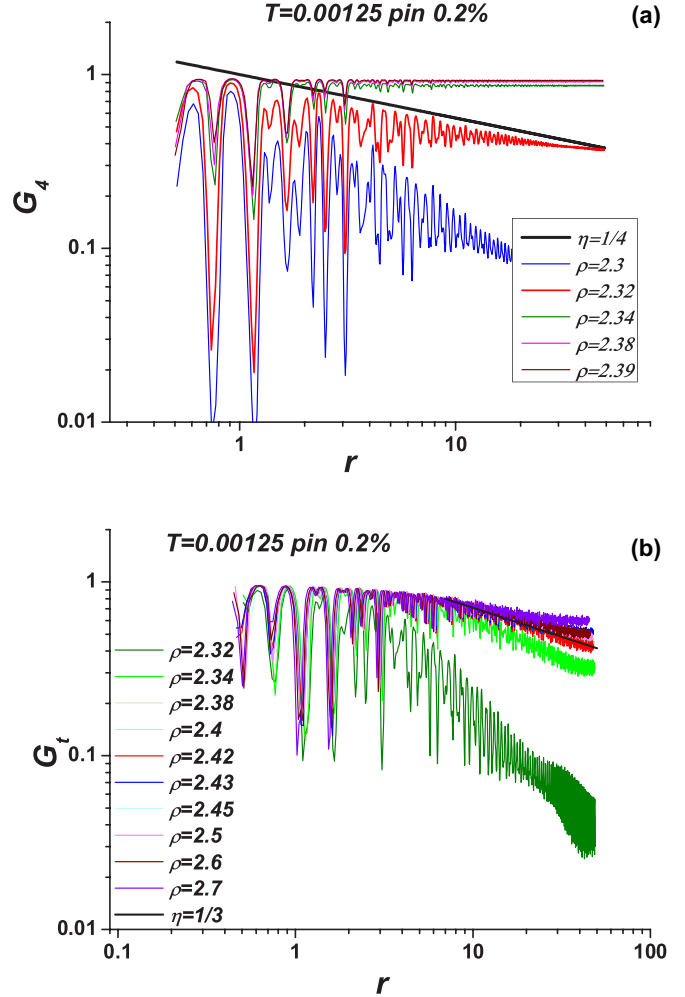

FIG. 8. (a) The orientational and (b) translational correlation functions with the symmetry of a square lattice with concentration of random pinning 0.2% in the region of transition from the triangular to square crystal at $T = 0.00125$.

Mayer-Wood loop and inside of it and do the same for the square one to the right of the loop and inside of it, respectively. Figure 7 shows the correlation functions corresponding to the triangular lattice. From these figures it is evident that at density $\rho = 2.26$ the triangular crystal loses stability and continually transitions according to BKT to the hexatic phase, which, in turn, loses stability at $\rho = 2.33$ that is inside the loop. An analogous situation arises for the square crystal: from the correlation functions in Fig. 8 it is evident that the tetratic stability limit is located inside the loop at $\rho = 2.32$, while the stability limit of the crystal itself is outside of it at $\rho = 2.42$, which is evidence of its continuous transition of the BKT type to the tetratic phase. Consequently, the loop itself corresponds to the hexatic-tetratic coexistence area and to the first-order transition between these phases owing to the basic difference of their orientational symmetry. With a further increase in density a continuous BKT transition from the tetratic phase to the square crystal takes place.

Thus in the presence of random pinning the scenario of transition between the two crystals changes fundamentally, in this case between the triangular and square crystals. Whereas in the system without random pinning

this transition occurs via a first-order phase transition, in the presence of random pinning transformation from the triangular crystal into the square one takes place via a whole cascade of transitions of a different nature. As was shown previously [64], random pinning could transform a first-order melting transition into two transitions corresponding to the third melting scenario. In the present case, one first-order structural transition changed into three transitions. First, the triangular crystal continuously transforms into the hexatic phase. After that, the hexatic phase transitions to tetratic via a first-order phase transition. Finally, the tetratic phase continuously transforms into the square crystal. This scenario is illustrated in Fig. 9.

It is noteworthy that the mechanism of transition between crystals detected by us in the presence of random pinning is in qualitative agreement with the influence of random pinning on crystal melting [64]. Random pinning destabilizes the crystal and expands the existence area of the hexatic (in the case of the square crystal, tetratic) phase. Moreover, the introduction of random pinning can generate the hexatic or tetratic phase if in the system without it melting took place by means of
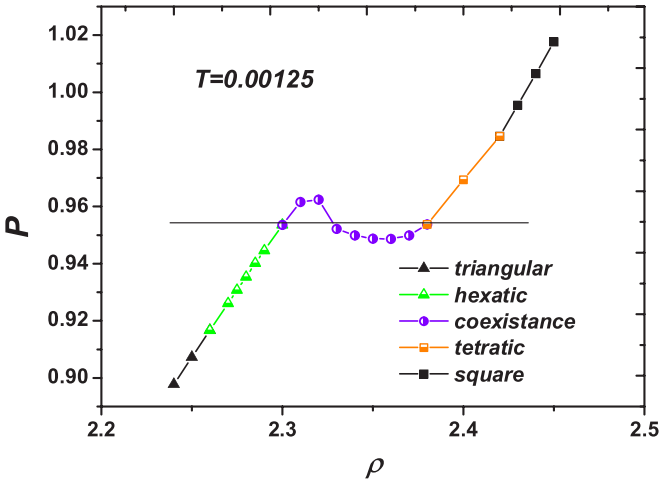
FIG. 9. The sequence of phases in transition from the triangular to square crystal in the system with 0.2% of random pinning at $T = 0.00125$.
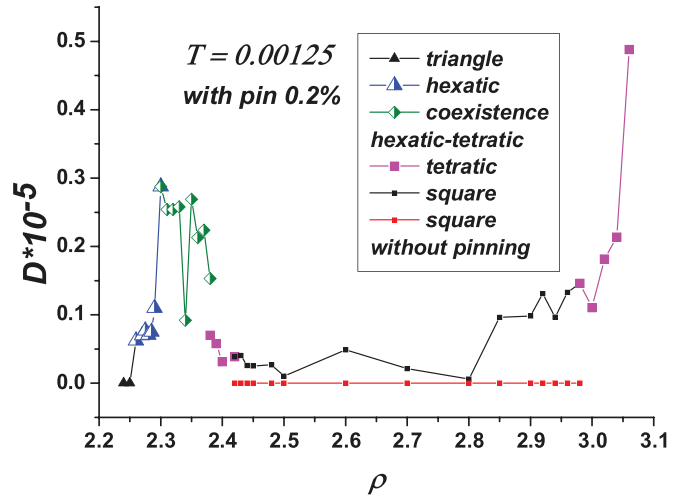

FIG. 10. Diffusion coefficient behavior depending on density in the system with pinning 0.2% and in the transition area between the triangular and square crystals at $T = 0.00125$.

first-order transition without the hexatic or tetratic phase. An example of such behavior is the right branch of square crystal melting in the system under investigation. Similarly, in transition from one crystal to another random pinning destabilizes the crystal before reaching the first-order transition line (the Mayer-Wood loop) and transforms it into the hexatic (tetratic for the square crystal) phase.

Figure 1 represents the phase diagram of Hertzian spheres both without random pinning and with random pinning with concentrations 0.1% and 0.2%, which reflects the given results and considerations. It should be noted that while in order to watch the influence of random pinning on the melting curve it was sufficient to add only 0.1% of fixed particles, to observe the influence of random pinning on transition between the crystals it was necessary to increase the concentration of fixed particles to 0.2%. This may be due to the fact that the overall mobility of the particles during transition from one crystal to another is lower than during melting of the system. To illustrate this, let us consider the behavior of the diffusion coefficient at $T = 0.00125$ in the density range from $\rho = 2.24$ to 3.06 (Fig. 10). The lowest densities of this range correspond to the triangular crystal, the highest, to the tetratic phase at the densities up to square crystal melting on the right branch. The values of the diffusion coefficient in the different phases are denoted by different symbols. As expected, in the crystals without random pinning the diffusion coefficient is near zero. On the introduction of random pinning, the diffusion coefficient becomes somewhat above zero, which is characteristic of crystals with defects. The diffusion coefficient sharply increases in the hexatic and tetratic phases as well as in the area of their coexistence.

Similar conclusions can be made from shear modulus behavior shown in Fig. 11. It is evident that the shear modulus has great importance in the crystalline phases. In transition to hexatic or tetratic the shear modulus falls sharply. Importantly, in the presented simulation the shear modulus in the hexatic and tetratic phases turns out to be more than zero, which is due to simulation limitations. However, it might become strictly zero after solving the renormalization group equations shown

in the Appendix. In the coexistence area of hexatic and tetratic the shear modulus becomes zero.

VI. CONCLUSIONS

We study the influence of random pinning on the phase diagram of 2D Hertzian spheres with $\alpha = 5/2$. The full phase diagram of a system with pinning in the existence area of the triangular and square crystals was built. It was shown that random pinning decreased the stability area of crystalline phases and increased the area of stability of the hexatic and tetratic phases as well as changing the melting scenario of the square crystal from one first-order transition to the third type of melting, which is in qualitative agreement with the previous works. For the first time, the influence of random pinning on transition between two crystalline phases was investigated. It was shown that the introduction of random
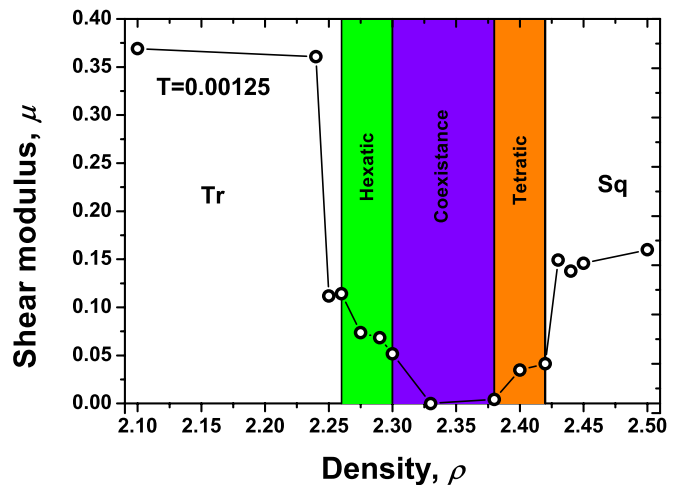

FIG. 11. The shear modulus depending on density in the system with pinning in the transition area between the triangular and square crystals at $T = 0.00125$.

pinning significantly changed the mechanism of transition. While in the system without random pinning transition took place as a first-order transition, the introduction of pinning makes it a three-stage one: the triangular crystal continuously transforms into hexatic, the hexatic via a first-order transition transforms into tetratic, after which the tetratic continuously transforms into the square crystal. This mechanism is in qualitative agreement with predictions on the influence of random pinning on the melting curve and may, in a certain sense, be considered as an extension of the BKTHNY melting mechanism to transition between two 2D crystalline phases.

APPENDIX

Of special interest is the influence of random pinning on the behavior of the triangular crystal melting curve near its maximum, which in the system without pinning takes place at density $\rho = 1.6$ [9]. As is seen in Fig. 1, without pinning the width of the hexatic phase tends to zero in the vicinity of the melting curve maximum. The point with maximum temperature T_{max} on the melting curve is a tricritical point in which the hexatic-liquid transition undergoes a change in the transition scenario from first order at $\rho < 1.6$ to continuous of the BKT type at $\rho > 1.6$. Can random pinning affect the value of T_{max}? In Fig. 12(a) isochores $\rho = 1.6$ are represented that, at first sight, fully coincide for the systems without and with pinning 0.1%. On both isochores the inflection point at $T = 0.0098$ is clearly seen that corresponds to the tricritical point in the system without pinning [9,11], and, as we suppose, in the system with pinning it will have the same value. Figure 12(b) shows the behavior of radial distribution functions $g(r)$ along isochore $\rho = 1.6$ for the system with pinning. From the figure it can be seen that with an increase in temperature the splitting of the second peak characteristic of the triangular crystal is blurred forming a single peak and at $T = 0.01$ the form of $g(r)$ corresponds to liquid. It can be supposed that the transition from hexatic to liquid based on the behavior criterion of $g(r)$ occurs at $T = 0.0098$, which is in full agreement with the data on the isochores.

However, these results do not provide information on the crystal-hexatic transition boundary. In order to determine the exact crystal-hexatic-liquid transition boundary we made use of the criterion on the basis of studying the orientational and translational order parameter correlation functions on isochore $\rho = 1.6$ at concentration of random pinning 0.1%, which are represented in Fig. 13. It can be seen that the crystal loses stability with respect to transition to hexatic at slightly above $T = 0.0078$, i.e., long before reaching the temperature of a maximum ($T_{max} = 0.0098$). Thus, the crystal finds itself
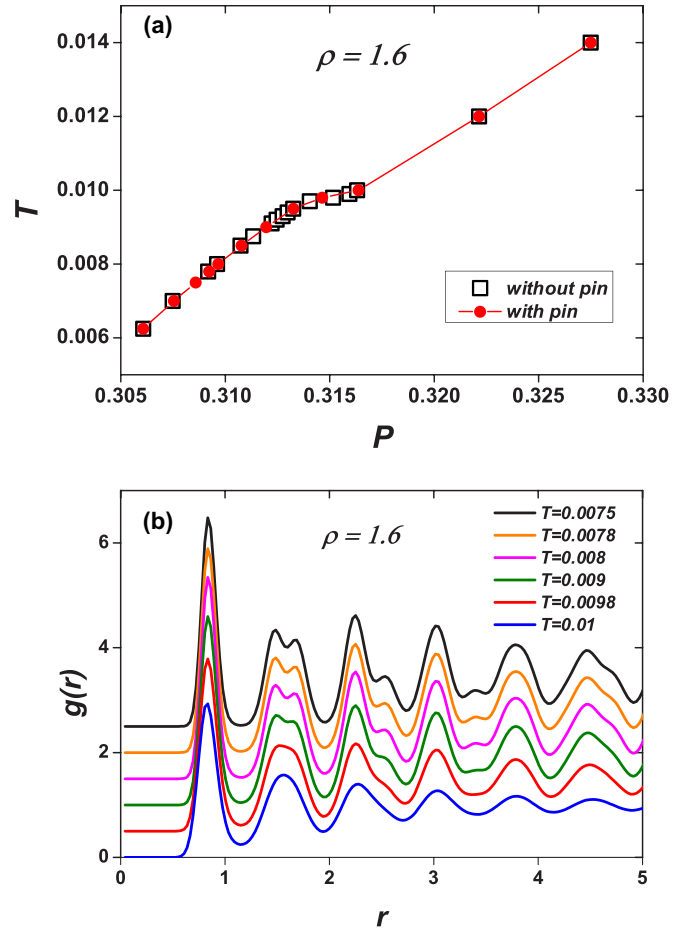

FIG. 12. (a) Isochores $\rho = 1.6$ for the system without pinning and in the presence of pinning 0.1%. (b) Radial distribution functions $g(r)$ for the system with pinning 0.1% as they approach the tricritical point. For better visualization, the curves are shifted along axis Y with a step of 0.5.

completely surrounded by the hexatic phase existence area. All three criteria with high accuracy yielded the value of the tricritical point at $T_{max} = 0.0098$. This result emphasizes once again that random pinning does not affect the orientational order parameter and its correlation function and, accordingly, the hexatic phase stability limit.

In order to additionally confirm a substantial decrease in crystal-hexatic transition temperature under the influence of pinning at density $\rho = 1.6$ we made use of the calculation and the renormalization procedure of the Young modulus presented in [24,68–70]. The elastic properties of a triangular crystalline lattice may be fully described by two independent elastic constants, namely, bulk modulus B and shear modulus μ. Shear modulus μ is calculated using the method suggested in [71]. In this method, the system is considered as strained. As a result, a nondiagonal pressure component appears that is proportional to the shear modulus:

$$P_{xy} = \mu u_{xy} + O(u_{xy}^2), \tag{A1}$$

where u_{xy} is strain. Figure 14 shows P_{xy} depending on the strain. It can be seen that in the crystal at low temperatures far from the point of transition to the hexatic phase the
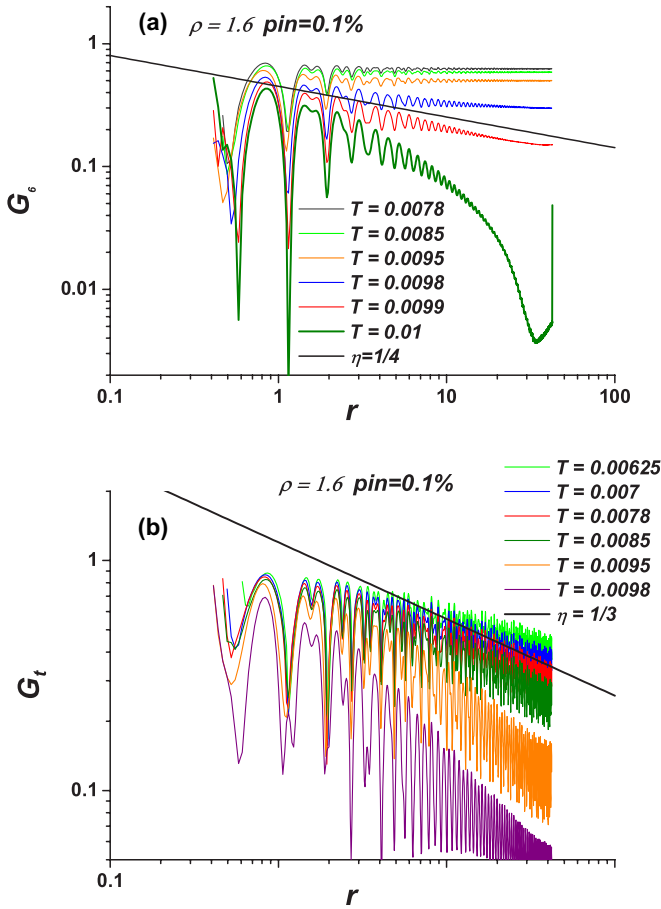
FIG. 13. (a) Orientational and (b) translational correlation functions G_6 and G_t along isochore $\rho = 1.6$ at random pinning concentration 0.1%.

dependence is characterized by strong linearity. The accuracy of calculations becomes worse when approaching transition to the hexatic phase.
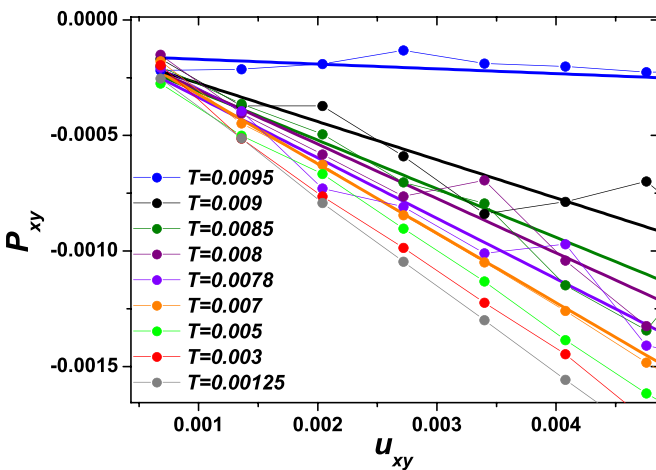

FIG. 14. The nondiagonal component of pressure as a function of applied strain along isochore $\rho = 1.6$ at random pinning concentration 0.1%.
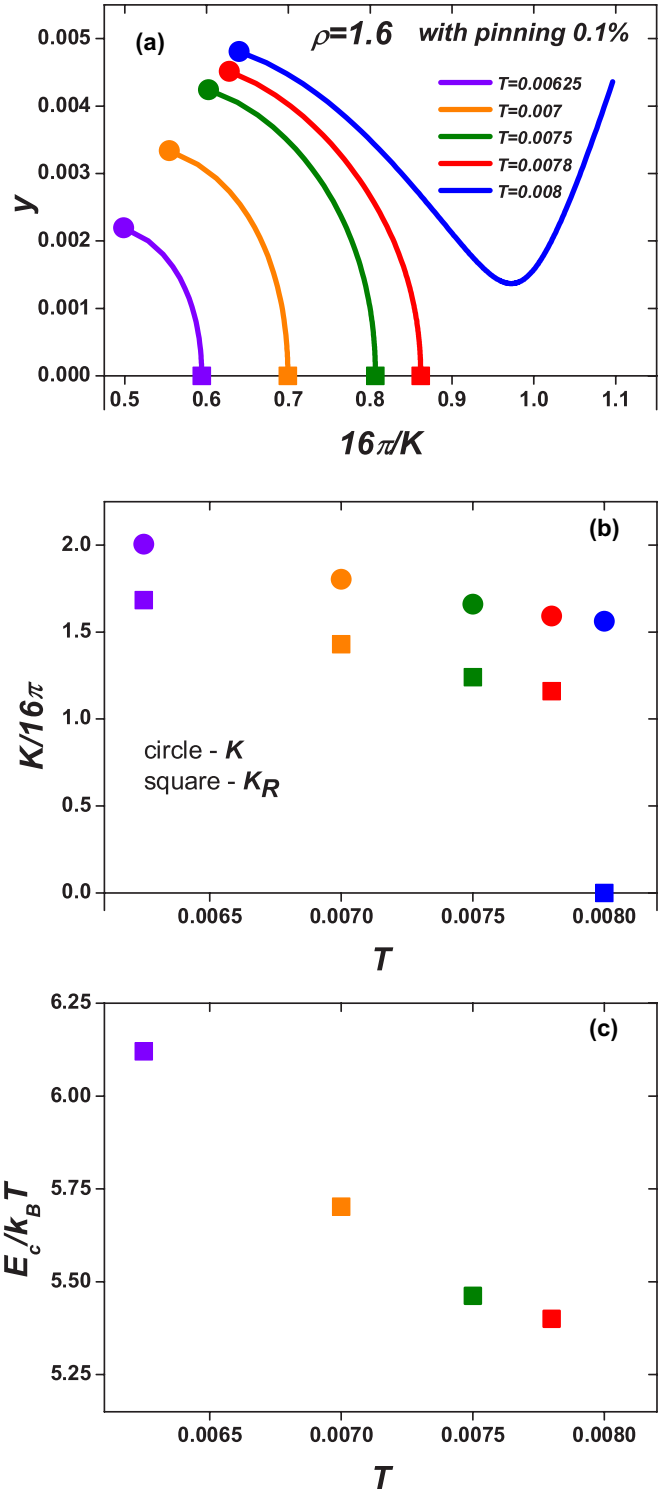

FIG. 15. (a) Trajectory $y - K$ as a result of renormalization for different temperatures at density $\rho = 1.6$ in the system with pinning 0.1%. (b) The unrenormalized K and renormalized K_R Young moduli depending on temperature for the same system. (c) Dimensionless energy of the dislocation core $E_c/k_B T$ depending on temperature for the same system.

Young's modulus K of a 2D triangular crystal that is a combination of bulk modulus B and shear modulus μ is calculated

from the relation

$$K = \frac{8}{\sqrt{3}\rho k_B T} \frac{\mu(\mu + \lambda)}{2\mu + \lambda}, \quad (A2)$$

where the Lame coefficient λ is connected with bulk modulus $B = (dP/d\rho)_T = \mu + \lambda$ [18,20,21]. The unrenormalized elastic constants and Young's modulus only make sense for an ideal defect-free triangular lattice. In the case of the presence of topological defects such as dislocations, the renormalization procedure is simply obligatory in accordance with the BKTHNY theory about a considerable decrease in elasticity in the presence of dislocations.

In order to renormalize Young's modulus, first, we determine dislocation core energy E_c [72] that is directly connected with the probability of detection of a dislocation pair:

$$p_d = \frac{16\sqrt{3}\pi^2}{K - 8\pi} I_0\left[\frac{K(l)}{8\pi}\right] e^{\frac{K(l)}{8\pi}} e^{-\frac{2E_c}{k_B T}}, \quad (A3)$$

where I_0 and I_1 are modified Bessel functions [72,73]. Note that $p_d = n_{dp}/N$, where n_{dp} is the number of dislocation pairs per the number of particles N. We renormalize Young's modulus and fugacity of dislocations y using the recursive equations [20,21]:

$$\frac{dK^{-1}(l)}{dl} = \frac{3\pi}{4} y^2(l) e^{\frac{K(l)}{8\pi}} \left\{ 2I_0\left[\frac{K(l)}{8\pi}\right] - I_1\left[\frac{K(l)}{8\pi}\right] \right\}, \quad (A4)$$

$$\frac{dy(l)}{dl} = \left[2 - \frac{K(l)}{8\pi}\right] y(l) + 2\pi y^2(l) e^{\frac{K(l)}{16\pi}} I_0\left[\frac{K(l)}{8\pi}\right], \quad (A5)$$

where l is the flowing number of renormalization group analysis. The limit of an infinite system corresponds to infinitely large l. Unrenormalized Young's modulus K ($l = 0$) and y ($l = 0$) = $\exp(-E_c/k_B T)$ serve as initial conditions for connected differential equations [Eqs. (A4) and (A5)].

Figure 15(a) shows the trajectories in plane y-K for different temperatures at density $\rho = 1.6$. The crystal loses stability when the curves leave for infinity generating an unordered hexatic phase. From Fig. 15(a) it is evident that this happens at temperature between $T = 0.0078$ and $T = 0.008$. At the same time according to the BKTHNY theory, renormalized Young's modulus K_R undergoes a sharp jump from 16π to 0, which is caused by the loss of shear resistivity. As shown in Fig. 15(b) the unrenormalized K and renormalized K_R Young moduli decrease with temperature growth up to $T = 0.0078$. Further temperature growth leads to a sharp fall of K_R to 0, i.e., the system transforms into the hexatic phase, which is in good agreement with the result from G_t. It is possible to conclude that both criteria are sensitive to formation of dislocation pairs. The dimensionless energy of the dislocation core shown in Fig. 15(c) at the crystal-hexatic transition point has value $E_c/k_B T = 5.4$, which is higher than $2.84k_B T$ in the case of first-order transition [15]. Hence, crystal-hexatic transition is due to dissociation of dislocation pairs and is a continuous transition of the BKT type. So from the collection of all criteria it is possible to say with confidence that in the system with pinning on tricritical isochore $\rho = 1.6$ the triangular crystal melts into the hexatic phase in accordance with the BKT theory. Random pinning significantly expanded the hexatic phase area at the expense of destruction of the crystal, but in no way did it affect the magnitude of tricritical temperature.

[1] C. N. Likos, Soft Matter **2**, 478 (2006).
[2] A. Fernandez-Nieves and A. M. Puertas, *Fluids, Colloids, and Soft Materials: An Introduction to Soft Matter Physics* (Wiley, New York, 2016).
[3] A. Ivlev, H. Lowen, G. Morfill, and C. P. Royall, *Complex Plasmas and Colloidal Dispersions: Particle-Resolved Studies of Classical Liquids and Solids, Series in Soft Condensed Matter* (Word Scientific, Singapore, 2012).
[4] L. Athanasopoulou and P. Ziherl, Soft Matter **13**, 1463 (2017).
[5] A. Suto, Phys. Rev. B: Condens. Matter Mater. Phys. **74**, 104117 (2006).
[6] C. N. Likos, Nature (London) **440**, 433 (2006).
[7] J. Pamies, A. Cacciuto, and D. Frenkel, J. Chem. Phys. **131**, 044514 (2009).
[8] E. N. Tsiok, E. A. Gaiduk, Y. D. Fomin, and V. N. Ryzhov, Soft Matter **16**, 3962 (2020).
[9] Y. D. Fomin, E. A. Gaiduk, E. N. Tsiok, and V. N. Ryzhov, Mol. Phys. **116**, 3258 (2018).
[10] W. L. Miller and A. Cacciuto, Soft Matter **7**, 7552 (2011).
[11] M. Zu, J. Liu, H. Tong, and N. Xu, Phys. Rev. Lett. **117**, 085702 (2016).
[12] M. Zu, P. Tan, and N. Xu, Nat. Commun. **8**, 2089 (2017).
[13] V. N. Ryzhov, E. E. Tareyeva, Y. D. Fomin, and E. N. Tsiok, Phys. Usp. **60**, 857 (2017).
[14] V. N. Ryzhov, E. E. Tareyeva, Y. D. Fomin, and E. N. Tsiok, Phys. Usp. **63**, 417 (2020).
[15] S. T. Chui, Phys. Rev. B: Condens. Matter Mater. Phys. **28**, 178 (1983).
[16] V. N. Ryzhov, ZhETF **100**, 1627 (1991) [JETP **73**, 899 (1991)].
[17] V. L. Berezinskii, ZhETF **59**, 907 (1971) [JETP **32**, 493 (1971)].
[18] J. M. Kosterlitz and D. J. Thouless, J. Phys. C **6**, 1181 (1973).
[19] B. I. Halperin and D. R. Nelson, Phys. Rev. Lett. **41**, 121 (1978).
[20] D. R. Nelson and B. I. Halperin, Phys. Rev. B **19**, 2457 (1979).
[21] A. Young, Phys. Rev. B **19**, 1855 (1979).
[22] E. P. Bernard and W. Krauth, Phys. Rev. Lett. **107**, 155704 (2011).
[23] M. Engel, J. A. Anderson, S. C. Glotzer, M. Isobe, E. P. Bernard, and W. Krauth, Phys. Rev. E **87**, 042134 (2013).
[24] W. Qi, A. P. Gantapara, and M. Dijkstra, Soft Matter **10**, 5449 (2014).
[25] S. C. Kapfer and W. Krauth, Phys. Rev. Lett. **114**, 035702 (2015).
[26] A. L. Thorneywork, J. L. Abbott, D. G. A. L. Aarts, and R. P. A. Dullens, Phys. Rev. Lett. **118**, 158001 (2017).
[27] K. S. Novoselov, A. K. Geim, S. V. Morozov, D. Jiang, Y. Zhang, S. V. Dubonos, I. V. Grigorieva, and A. A. Firsov, Science **306**, 666 (2004).

[28] G. Algara-Siller, O. Lehtinen, F. C. Wang, R. R. Nair, U. Kaiser, H. A. Wu, A. K. Geim, and I. V. Grigorieva, Nature (London) **519**, 443 (2015).

[29] J. Zhao, Q. Deng, A. Bachmatiuk, G. Sandeep, A. Popov, J. Eckert, and M. H. Rümmeli, Science **343**, 1228 (2014).

[30] N. Osterman, D. Babic, I. Poberaj, J. Dobnikar, and P. Ziherl, Phys. Rev. Lett. **99**, 248301 (2007).

[31] C. A. Bolle, P. L. Gammel, D. G. Grier, C. A. Murray, D. J. Bishop, D. B. Mitzi, and A. Kapitulnik, Phys. Rev. Lett. **66**, 112 (1991).

[32] S. J. Ray, A. S. Gibbs, S. J. Bending, P. J. Curran, E. Babaev, C. Baines, A. P. Mackenzie, and S. L. Lee, Phys. Rev. B **89**, 094504 (2014).

[33] F. Leoni and G. Franzese, J. Chem. Phys. **141**, 174501 (2014).

[34] S. A. Rice, Chem. Phys. Lett. **479**, 1 (2009).

[35] Z. Krebs, A. B. Roitman, L. M. Nowack, C. Liepold, B. Lin, and S. A. Rice, J. Chem. Phys. **149**, 034503 (2018).

[36] E. N. Tsiok, Y. D. Fomin, and V. N. Ryzhov, Physica A **550**, 124521 (2020).

[37] L. A. Padilla and A. Ramirez-Hernandez, J. Phys.: Condens. Matter **32**, 275103 (2020).

[38] D. S. Cardoso, V. F. Hernandes, T. P. O. Nogueira, and J. R. Bordin, Physica A **566**, 125628 (2021)

[39] O. Vilanova and G. Franzese, arXiv:1102.2864.

[40] F. Martelli, H.-Y. Ko, C. Calero, and G. Franzese, Front. Phys. **13**, 136801 (2018).

[41] M. M. Marques, N. P. O. Nogueira, R. R. Dillenburg, M. C. Barbosa, and J. R. Bordin, J. Appl. Phys. **127**, 054701 (2020).

[42] J. R. Bordin and M. C. Barbosa, Phys. Rev. E **97**, 022604 (2018).

[43] L. Nowack and S. A. Rice, J. Chem. Phys. **151**, 244504 (2019).

[44] D. E. Dudalov, Y. D. Fomin, E. N. Tsiok, and V. N. Ryzhov, J. Phys. Conf. Ser. **510**, 012016 (2014).

[45] D. E. Dudalov, Y. D. Fomin, E. N. Tsiok, and V. N. Ryzhov, J. Chem. Phys. **141**, 18C522 (2014).

[46] D. E. Dudalov, Y. D. Fomin, E. N. Tsiok, and V. N. Ryzhov, Soft Matter **10**, 4966 (2014).

[47] A. Jain, J. R. Errington, and T. M. Truskett, Phys. Rev. X **4**, 031049 (2014).

[48] E. Marcotte, F. H. Stillinger, and S. Torquato, J. Chem. Phys. **134**, 164105 (2011).

[49] W. D. Pineros, M. Baldea, and T. M. Truskett, J. Chem. Phys. **145**, 054901 (2016).

[50] M. Engel and H.-R. Trebin, Phys. Rev. Lett. **98**, 225505 (2007).

[51] T. Dotera, T. Oshiro, and P. Ziherl, Nature (London) **506**, 208 (2014).

[52] H. Pattabhiraman and M. Dijkstra, J. Chem. Phys. **146**, 114901 (2017).

[53] N. P. Kryuchkov, S. O. Yurchenko, Y. D. Fomin, E. N. Tsiok, and V. N. Ryzhov, Soft Matter **14**, 2152 (2018).

[54] D. R. Nelson, Phys. Rev. B **27**, 2902 (1983).

[55] S. Sachdev and D. R. Nelson, J. Phys. C **17**, 5473 (1984).

[56] M. C. Cha and H. A. Fertig, Phys. Rev. Lett. **74**, 4867 (1995).

[57] S. Herrera-Velarde and H. H. von Grunberg, Soft Matter **5**, 391 (2009).

[58] E. A. Gaiduk, Y. D. Fomin, E. N. Tsiok, and V. N. Ryzhov, Mol. Phys. **117**, 2910 (2019)

[59] E. N. Tsiok, Y. D. Fomin, and V. N. Ryzhov, Physica A **490**, 819 (2018).

[60] T. Horn, S. Deutschlander, H. Lowen, G. Maret, and P. Keim, Phys. Rev. E **88**, 062305 (2013).

[61] S. Deutschlander, T. Horn, H. Lowen, G. Maret, and P. Keim, Phys. Rev. Lett. **111**, 098301 (2013).

[62] K. Zahn, R. Lenke, and G. Maret, Phys. Rev. Lett. **82**, 2721 (1999).

[63] W. Qi and M. Dijkstra, Soft Matter **11**, 2852 (2015).

[64] E. N. Tsiok, D. E. Dudalov, Y. D. Fomin, and V. N. Ryzhov, Phys. Rev. E **92**, 032110 (2015).

[65] L. D. Landau and E. M. Lifshitz, *Theory of Elasticity*, 3rd ed. (Pergamon, New York, 1986).

[66] Y. D. Fomin, V. N. Ryzhov, and N. V. Gribova, Phys. Rev. E **81**, 061201 (2010).

[67] http://lammps.sandia.gov/; S. Plimpton, J. Comp. Phys. **117**, 1 (1995).

[68] J. R. Ray, Comput. Phys. Rep. **8**, 109 (1988).

[69] J. Lutsko, J. Appl. Phys. **65**, 2991 (1989).

[70] E. Voyiatzis, Comput. Phys. Commun. **184**, 27 (2013).

[71] J. Q. Broughton, G. H. Gilmer, and J. D. Weeks, Phys. Rev. B **25**, 4651 (1982).

[72] S. Sengupta, P. Nielaba, and K. Binder, Phys. Rev. E **61**, 6294 (2000).

[73] D. S. Fisher, B. I. Halperin, and R. Morf, Phys. Rev. B **20**, 4692 (1979).